

**This item is the archived peer-reviewed author-version of:**

Scleral asymmetry as a potential predictor for scleral lens compression

**Reference:**

Consejo Alejandra, Behaegel Joséphine, Van Hoey Maarten, Iskander D. Robert, Rozema Jos.- Scleral asymmetry as a potential predictor for scleral lens compression

Ophthalmic and physiological optics - ISSN 0275-5408 - 38:6(2018), p. 609-616

Full text (Publisher's DOI): <https://doi.org/10.1111/OPO.12587>

To cite this reference: <https://hdl.handle.net/10067/1564680151162165141>

# Scleral asymmetry as a potential predictor for scleral lens compression

Alejandra Consejo<sup>1,2,3\*</sup>, Joséphine Behaegel<sup>2,4</sup>, Maarten Van Hoey<sup>1</sup>, D. Robert Iskander<sup>3</sup> and  
Jos J. Rozema<sup>1,2</sup>

<sup>1</sup> Department of Ophthalmology, Antwerp University Hospital, Edegem, Belgium

<sup>2</sup> Department of Medicine and Health Sciences, University of Antwerp, Antwerp, Belgium

<sup>3</sup> Department of Biomedical Engineering, Wrocław University of Science and Technology, Wrocław, Poland

<sup>4</sup> Department of Ophthalmology, Brussels University Hospital, Jette, Belgium

## ABSTRACT

**Purpose:** To identify the position and magnitude of lens compression due to short-term miniscleral contact lens wear, as well as evaluating the usefulness of scleral asymmetry as a predictor for scleral lens decentered compression.

**Methods:** Fourteen healthy subjects (mean  $\pm$  SD: 29.2  $\pm$  6.0 years) wore a highly gas-permeable miniscleral contact lens during a 5-hour period. Corneo-scleral height Fourier profilometry (Eye Surface Profiler) was captured before and immediately after lens removal. Scleral asymmetry, lens compression location and magnitude were processed using custom-made algorithms, both globally and for scleral quadrants.

**Results:** Miniscleral contact lenses do not set uniformly on the ocular surface, with the largest decentration seen along the horizontal meridian. The greatest flexural stress exerted by the lens on the ocular surface occurs at the point coinciding with the inner diameter landing point of the lens and not with its overall diameter. Scleral asymmetry was significantly correlated with compression location ( $R = 0.71$ ,  $p = 0.002$ ) and compression magnitude ( $R = 0.81$ ,  $p < 0.001$ ), showing its potential as compression predictor.

**Conclusion:** Larger amounts of scleral asymmetry will lead to more scleral lens decentration. Objective and accurate methods, like the one presented here, could help the practitioner prevent cases of scleral blanching or discomfort due to an excessive compression by the lens.

## KEYWORDS

Miniscleral contact lens; anterior eye surface; corneo-scleral topography; impingement; lens compression

## DISCLOSURE

The authors report no conflicts of interest and have no proprietary interest in any of the materials mentioned in this article.

## ACKNOWLEDGEMENTS

This work was supported by the Polish National Science Centre; Preludium grant, 2016/21/N/ST7/02298. The authors thank Microlens Contactlens Technology b.v. (Arnhem, The Netherlands) for providing the contact lenses used in this study.

## INTRODUCTION

Scleral contact lenses have repeatedly shown to improve visual acuity, vision-related quality of life and ocular surface integrity in irregular corneal topographies in a range of ocular surface diseases.<sup>1</sup> The scleral lens market has seen a great boost over the last years, stimulated by advances in ophthalmic instrumentation and the increased interest of practitioners that wish to expand their scleral contact lens fitting skills.<sup>2</sup>

As scleral lenses become more popular, practitioners gain more interest in assessing the anterior scleral shape.<sup>3-6</sup> Scleral asymmetry, undesired lens seal-off and limbal bearing are some of the main fitting challenges associated with scleral contact lenses.<sup>7</sup> Scleral asymmetry may result in an uneven distribution of the pressure exerted by the lens ('lens load'), leading to an uneven scleral compression across sectors. For example, scleral flattening resulting from short-term scleral contact lens wear was found to be not uniformly distributed, with the greatest scleral flattening observed in the superior sector. This phenomenon was observed using Optical Coherence Tomography (OCT)<sup>8</sup> and more recently, corneo-scleral profilometry.<sup>9</sup> Such an unequal weight bearing of the lens could lead to sectorial impingement and compression of the conjunctiva, especially in highly irregular scleras.<sup>7</sup> Similarly, it was recently shown that scleral asymmetry is associated with scleral lens flexure.<sup>10</sup>

Scleral shape has also been identified as a potential factor causing the inferior temporal decentration seen in most spherical haptic scleral lenses, along with gravity and eyelid forces during blinking.<sup>3,11</sup> This decentration may cause performance issue with newer lens types, such as multifocal or wavefront guided scleral lenses.<sup>12</sup> This issue will likely deteriorate in the presence of scleral asymmetry as it may lead to uneven compression and consequently lens decentration, although this relationship has not yet been firmly established.

The present study was designed to gain greater understanding on how scleral shape relates with scleral lens compression. To this end we first present an automatic method to quantify scleral asymmetry based on 3-dimensional (3D) scleral profilometry maps, which are then analysed to establish the usefulness of scleral asymmetry as a potential predictor for the location and amplitude of scleral lens compression.

## METHODS

This study was approved by the Antwerp University Hospital Research Ethics Committee and adhered to the tenets of the Declaration of Helsinki. All subjects gave written informed consent to participate after the nature and possible consequences of the study were explained. Participants in this study included 14 young, healthy adult subjects (11 females, three males) aged  $29.2 \pm 6.0$  years old (mean  $\pm$  standard deviation).

Given that previous studies using a similar experimental design (assessment of corneo-scleral topography before and after short-term scleral contact lenses using Fourier profilometry<sup>9</sup> or OCT<sup>8</sup>) reported statistically significant changes in corneo-scleral shape with sample sizes between 10 and 12, we selected a similar sample size for this study. This sample size guarantees detecting scleral elevation changes of  $\pm 30 \mu\text{m}$  at a 5% level of significance with 80% power.<sup>9</sup>

Prior to inclusion, all subjects were screened to exclude individuals with any contraindications to contact lens wear, such as significant tear film or anterior segment abnormalities. All participants were contact lens neophytes, except for three occasional soft contact lens wearers. These three individuals discontinued lens wear for at least 24 hours before participating to minimize the influence of soft lens wear on the ocular surface. None of the subjects has a history of prior rigid contact lens wear, ocular surgery or the current use of topical ocular medications, as reported by the participants in a background questionnaire.

### *Contact lens fitting*

Contact lens fitting was performed by an experienced optometrist (MVH). The lens design used was the spherical haptic landing zone miniMISA miniscleral lens, provided by Microlens (Arnhem, The Netherlands). The lenses were made of highly gas-permeable materials with a Dk of 125, central thickness of 300  $\mu\text{m}$ , and overall diameter of 16.5 mm, inner diameter landing point of 13.0 mm, back optical zone radius of 7.8 mm and landing zone radius of 13.5 mm. Two of the participants wore a miniscleral lens with an overall diameter of 17.0 mm and inner diameter landing point of 14.0 mm, with the rest of lens design parameters remaining the same. Individual analysis of these two subjects is undertaken in the Results section.

Lens fitting was conducted on the same day to data collection. The lens was placed onto a randomly chosen eye in each participant with preservative free saline solution. After placement its position was assessed using a slit lamp. If regions of corneal bearing were observed, the sagittal depth of the lens was increased in 125  $\mu\text{m}$  increments and the fit reassessed. If a potential participant had been unable to wear the described miniscleral lens of 16.5 or 17.0 mm overall diameter, the participant would have withdrawn the study. Central corneal clearance was assessed immediately after lens insertion and after 5 hours of lens settling, using an anterior spectral domain OCT (RTVue, Optovue Inc., Fremont, CA, USA). The callipers within the analysis software were used to determine the distance between the back surface of the miniscleral contact lens and the anterior surface of the cornea to provide a measure of the central corneal clearance at the position of the corneal reflex. Limbal clearance was observed using slit lamp examination.

### *Measurements and data collection*

The study was conducted in two sessions on the same day. Each session included six measurements from the eye where the miniscleral lens was inserted with a corneo-scleral profilometer (Eye Surface Profiler (ESP), Eaglet Eye BV, Netherlands) that measures the corneo-scleral topography far beyond the limbus. These measurements require the instillation of fluorescein, which was done using BioGlo ophthalmic strips (HUB Pharmaceuticals), gently touching the upper temporal of the ocular surface after impregnation with 1 mg of fluorescein sodium ophthalmic moistened with one drop of an eye lubricant (HYLO-Parin, 1mg/ml of sodium hyaluronate). Subjects were instructed to open their eyes wide during measurements to ensure full coverage of the corneo-scleral area. Measurements for which part of the corneo-scleral area was covered by the eyelids were excluded.

Baseline measurements were conducted in the morning right before contact lenses insertion (0h, session 1, baseline measurements (MB)), with a minimum of two hours after waking to control the influence of diurnal variations in corneal topography.<sup>13</sup> The follow-up measurements were taken immediately after lens removal following five hours of wear (session 2, M5). After lens removal the eye was re-examined using a slit-lamp. Participants continued their normal daily activities between measurement sessions, in most cases standard office and computer work.

## Data analysis

After data acquisition, the raw anterior eye height data (three columns with  $X$ ,  $Y$ , and  $Z$  coordinates) were exported from the ESP for further analysis. The ESP device incorporates an internal procedure, based on 3-dimensional data, to estimate the position of the corneal apex and to correct corneal tilt or rotation (for details on the alignment procedure see <sup>14</sup>). This internal procedure also assures that all 3D maps are equally centred.

The compression location was estimated by assessing the 3D-topographical maps before (baseline, MB) and immediately after lens removal (M5). Each 3D map was split up in 0.1 mm-wide concentric annuli, starting at the corneal apex to the scleral periphery at 7.5 mm from the apex. The elevation change between the baseline (MB) and after lens wear (M5) was calculated for each of these rings. Maximum compression location was defined by the ring with the largest difference between elevation maps (M5-MB). Meanwhile, compression decentration was calculated as the difference between the estimated compression position and the projected compression position according to the manufacturer, i.e. at 6.5 mm radius for the subjects that wore a 16.5 mm overall diameter lens with a 13.0 mm inner diameter landing point and at 7.0 mm radius for the two subjects that wore a 17.0 mm overall diameter lens with a 14.0 mm inner diameter landing point. Furthermore, the sclera was divided into four quadrants: superior ( $45,135^\circ$ ), inferior ( $225,315^\circ$ ), nasal ( $135,225^\circ$ ) and temporal ( $315,45^\circ$ ), allowing to repeat this analysis for each sector. Eyes were corrected for mirror symmetry.

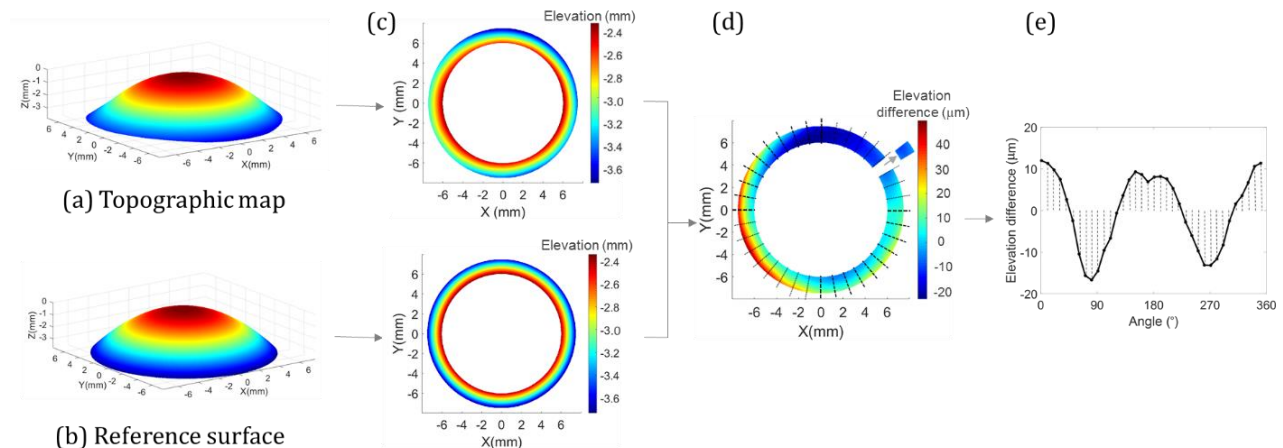


**Figure 1.** Schema illustrating the followed steps to estimate scleral asymmetry from 3D corneo-scleral topographic maps (a) and a conic quadratic reference surface (b). The difference between the corresponding scleral rings (c) was calculated (d). Further, a  $10^\circ$  sectorial division was done and RMS calculated (e) as an estimate of scleral asymmetry.

To estimate the magnitude of the scleral asymmetry the difference between the baseline 3D corneo-scleral topographies and a fixed reference surface was used. Figure 1 illustrates the methodology followed. First, raw 3D maps were imputed (Figure 1a), after which a reference surface was built using a conic quadratic function (Figure 1b). Next, the sclera and the cornea were automatically separated at the level of the limbus,<sup>15</sup> assuming a mean limbal diameter of 12 mm (Figure 1c).<sup>16</sup> The difference between the raw scleral annulus (Figure 1c up) and the corresponding annulus of reference surface (Figure 1c below) was calculated (Figure 1d). Furthermore, the scleral annulus of the elevation difference was divided in  $10^\circ$  sectors (Figure 1d), allowing the calculation of the

mean elevation difference in each sector (Figure 1e). Finally, scleral asymmetry was calculated in micrometres as the root mean square (RMS) of the elevation difference every  $10^\circ$  (Figure 1e). This procedure was repeated for the 6 baseline measurements acquired for every participant. To assess the repeatability of this methodology the Coefficient of Variation (CoV) was calculated. Moreover, scleral toricity was calculated as the greatest difference in scleral sagittal height between two perpendicular meridians.<sup>10</sup>

The statistical analysis was performed using SPSS software for Windows version 24.0 (SPSS Inc., Chicago, Illinois, United States). The Shapiro-Wilk test was used to test the distribution type (Gaussian or non-Gaussian) of all continuous variables, which confirmed the normality of all parameters ( $p > 0.05$ ). The level of significance was set to 0.05.

## RESULTS

The average location of the highest scleral flattening approximately coincides with the 6.5 mm inner radius landing point of the miniscleral lens worn by 12 participants (Figure 2). The average compression at this point was  $-130 \pm 50 \mu\text{m}$ . However, radial differences were observed between sectors (Table 1). The largest compression decentration from the apex was found in temporal and inferior sectors. The magnitude of lens compression was also not uniform between sectors, as the superior and temporal sectors were more affected by lens compression. Regional differences are illustrated by the example presented in Figure 3. The regional differences found were consistent with the results of the two participants that wore a larger miniscleral lens (inner diameter landing point 14.0 mm and overall diameter 17.0 mm). Here the average compression position on the temporal sector (mean  $\pm$  SD:  $7.3 \pm 0.05$  mm) was further from the apex than in the nasal sector (mean  $\pm$  SD:  $6.8 \pm 0.15$  mm). Similarly, the average compression position in superior sector (mean  $\pm$  SD:  $6.9 \pm 0.05$  mm) was closer to the apex than that in the inferior sector (mean  $\pm$  SD:  $7.2 \pm 0.15$  mm).

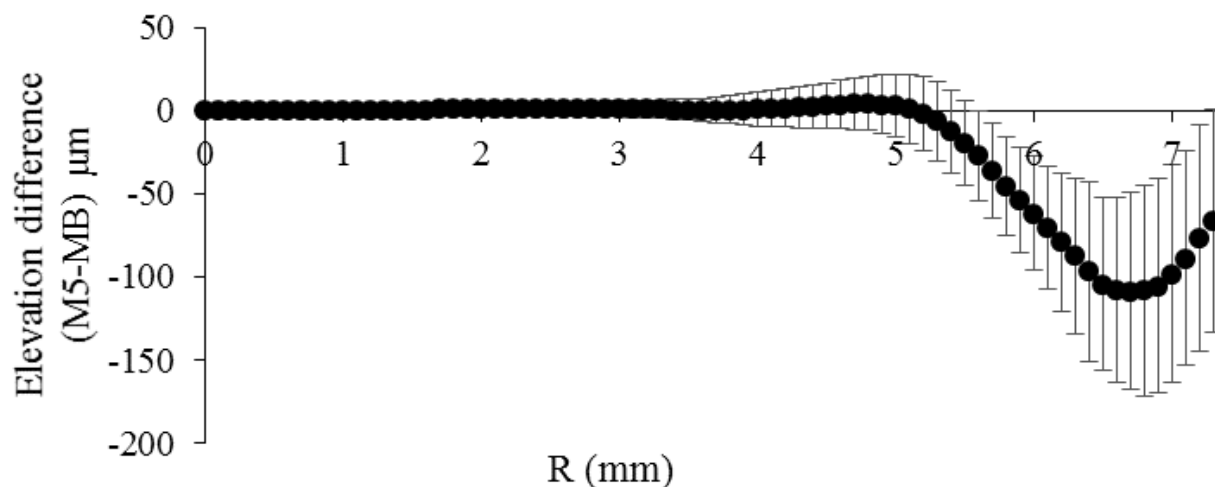


**Figure 2.** The mean elevation scleral difference between baseline (MB) and after lens removal measurements (M5) in 12 eyes wearing a miniscleral lens of 16.5 mm overall diameter and 6.5 mm inner radius landing point. Each point corresponds to the mean elevation in a 0.1 mm wide annulus, from corneal centre ( $R = 0$  mm) to scleral periphery ( $R > 7$  mm). Error bars indicate  $\pm 1$ SD

**Table 1.** Maximum compression location and maximum lens compression value per quadrant in 12 eyes wearing a miniscleral lens of 16.5 mm overall diameter and 6.5 mm inner radius landing point.

Sector	Mean maximum compression position (mm)	Mean scleral flattening in maximum compression position ( $\mu\text{m}$ )
Temporal	$6.69 \pm 0.40$	$170 \pm 90$
Nasal	$6.25 \pm 0.59$	$77 \pm 36$
Superior	$6.47 \pm 0.34$	$210 \pm 105$
Inferior	$6.66 \pm 0.21$	$95 \pm 62$

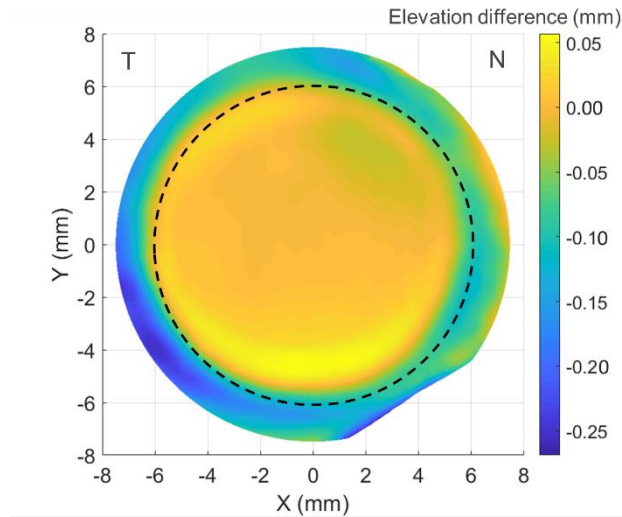


**Figure 3.** Example of the elevation difference map obtained subtracting the baseline topography (MB) from the topography acquired immediately after lens removal (M5), i.e. M5-MB, for a female subject that wore a 16.5mm-overall diameter miniscleral lens during a 5-hour period on her right eye. The black dashed line represents a 6.5 mm radius circle, corresponding to the position where lens compression would be expected to be found assuming a regular and symmetrical lens indentation.

A positive statistically significant correlation was found between scleral asymmetry and compression decentration ( $R = 0.71$ ;  $p = 0.002$ ; Figure 4), suggesting that the more asymmetric the sclera, the more the lens will be displaced from the expected landing position, i.e. 6.5 mm for the subjects that wore a 16.5 mm overall diameter lens, and 7.0 mm for the two subjects that wore a 17.0 mm overall diameter lens. Similarly, a positive, statistically significant correlation was found between scleral asymmetry and compression magnitude ( $R = 0.81$ ;  $p < 0.001$ ; Figure 5), suggesting more scleral asymmetry leads to more compression. Compression decentration and magnitude were also positively correlated ( $R = 0.64$ ;  $p = 0.007$ ), suggesting that larger compression decentration goes accompanied with larger scleral compression.

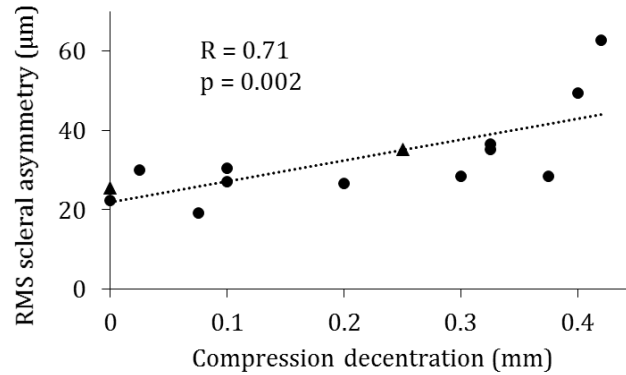


**Figure 4.** Correlation between scleral asymmetry, expressed in  $\mu\text{m}$ , and compression decentration for 14 subjects that wore a miniscleral lens during a 5-hour period. Circular markers represent participants who wore a 16.5 mm diameter lens, while triangular markers represent the two participants who wore a 17.0 mm diameter lens.

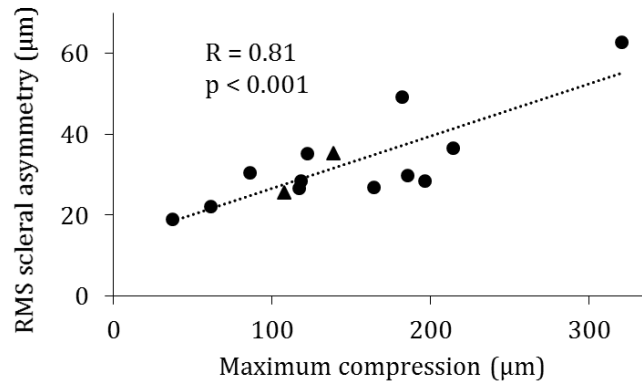


**Figure 5.** Correlation between scleral asymmetry, expressed in  $\mu\text{m}$ , and maximum compression for 14 subjects that wore a miniscleral lens during a 5-hour period. Circular markers represent participants who wore a 16.5 mm overall diameter lens, while triangular markers represent the two participants who wore a 17.0 mm overall diameter lens.

The mean initial central corneal clearance was  $330 \pm 80 \mu\text{m}$ , which reduced to  $260 \pm 80 \mu\text{m}$  after five hours of lens settling. A significant positive correlation was found between initial central corneal clearance and compression decentration ( $R = 0.65$ ,  $p = 0.02$ ). Similarly, a significant positive correlation was found between initial central corneal clearance and compression magnitude ( $R = 0.61$ ,  $p = 0.03$ ). These correlations indicate that lower initial central corneal clearance values were associated with lower compression effect. A weak positive correlation, close to statistically significance, was found between indentation decentration and corneal clearance decrease after five hours of lens settling ( $R = 0.44$ ,  $p = 0.08$ ). This correlation suggests that the larger reductions in central clearance are associated with more lens decentration.

The quantification of the scleral asymmetry for each individual subject (for details see Figure 1) showed a good repeatability. The CoV, calculated using the 6 repeated baseline measurements amounted on average to 6.2 % (range, 0.3% - 11.7%), which can be considered as a low-variance method.



The mean scleral toricity over a 15 mm length calculated as the greatest difference in scleral sagittal height between two perpendicular meridians amounted on average to  $200 \pm 100 \mu\text{m}$  (range 77 – 450  $\mu\text{m}$ ). This parameter positively correlated with maximum compression ( $R = 0.59$ ,  $p = 0.01$ ), but did not correlate well with compression decentration ( $R = 0.30$ ,  $p = 0.14$ ).

## DISCUSSION

In this study, scleral asymmetry showed its potential to be used as a parameter to predict scleral lens settling. Larger amounts of scleral asymmetry were found to lead to larger decentration in the impression of the lens on the ocular surface (Figure 4), as well as deeper compression of the sclera (Figure 5). Scleral asymmetry has repeatedly been mentioned as an important factor for a successful scleral lens fit.<sup>3,7</sup> This is the first work that shows an automatic methodology to quantify scleral asymmetry as single parameter that is correlated with lens compression. Compression was observed in all the cases analysed, ranging from 40 to 320  $\mu\text{m}$ . However, no corneal or conjunctival staining was observed with slit-lamp examination after lens removal. Interestingly, these results suggest that the greatest flexural stress exerted by the lens on the ocular surface occurs at the point coinciding with the inner diameter landing point of the lens and not with its overall diameter, independently from the overall diameter of the lens.

For consistency with existing literature, scleral toricity was also calculated only using two perpendicular meridians.<sup>4,10</sup> Vincent et al. reported a mean scleral toricity of  $198 \pm 140 \mu\text{m}$  over a 15 mm chord length, calculated over 9 healthy subjects measured with the same corneo-scleral topographer used in this work.<sup>10</sup> We obtained an average scleral toricity of  $220 \pm 100 \mu\text{m}$  calculated over the same chord distance, which is a good agreement. We did however observe that scleral toricity calculated this way is a poorer predictor of scleral lens compression than the automatic methodology presented in this work that considers the whole 3D scleral map, instead of only two meridians, to make an estimate of scleral asymmetry (Figure 1).

Different clinical studies noted the tendency of scleral contact lenses to decentre.<sup>11,17</sup> In a qualitative study based on slit-lamp examination on a large cohort, infero-temporal decentration was the most prevalent, followed by inferior and temporal decentration.<sup>17</sup> Significant temporal and inferior decentration (on average 0.18 mm and 0.20 mm, respectively) were found in a more recent work by Vincent et al., using an objective method based on OCT images.<sup>11</sup> Even though in this work we investigated compression rather than lens decentration, our findings are in line with these previous works. Significant compression decentration was observed across sectors (Table 1). A mean compression position of  $6.69 \pm 0.40 \text{ mm}$  in the temporal and  $6.66 \pm 0.21 \text{ mm}$  in the inferior sectors resulted in a compression decentration of 0.19 mm temporally and 0.16 mm nasally. Compression decentration was found to be larger in the horizontal meridian than in the vertical one.

Lower initial central corneal clearance values were associated with lower lens compression. Both compression decentration and compression magnitude were significantly positively correlated with initial central corneal clearance. These results are in accordance with the study performed by Esen et al.<sup>18</sup> They tested three different mini-scleral lenses with successively greater sagittal depths to achieve three levels of initial central corneal clearance and found that settling rate was significantly lower in low apical clearance group. Likewise, Vincent et al.<sup>11</sup> reported that lower initial central corneal clearance was associated with less horizontal miniscleral lens decentration. The mean

change in central corneal clearance after 5 hours of lens wear ( $-70 \pm 20 \mu\text{m}$ ) was similar to previous studies using miniscleral lenses of similar diameter.<sup>11,18,19</sup>

Conjunctival hyperemia and scleral blanching are unwanted phenomena often associated with scleral lens wear. Impingement compression of the conjunctiva to the point where the blood vessels are closed off is an undesirable outcome that will most likely have an effect on wearing time and comfort.<sup>6</sup> Patients that experience discomfort along with conjunctival hyperemia after extended hours of daily scleral lens wear might eventually reduce wearing time and even develop scleral lens intolerance. It is estimated that around ten percent of scleral contact lens wearers eventually discontinue lens wear due to discomfort.<sup>20,21</sup> These undesirable outcomes of scleral lens wear are often assessed using slit-lamp examination, which may be supplemented by the method presented here to objectively quantify these phenomena.

Comfort and safety of the contact lens wearer are greatly influenced by the interaction between the contact lens and the ocular surface.<sup>22,23</sup> Previous works evaluating the effect of scleral contact lenses on the ocular surface were mainly done with Scheimpflug cameras<sup>24-27</sup> or OCT.<sup>8,11</sup> The main limitation of Scheimpflug cameras is that their range of measurement is restricted to the cornea, while OCT analysis is limited to selected meridians so that precise repeatable alignment between measurements cannot be guaranteed. To overcome these limitations we used corneo-scleral profilometry, an alternative imaging technique able to simultaneously measure the cornea and the sclera in 3D along all meridians.<sup>28</sup> Corneo-scleral profilometry accounts for topographic changes in corneo-scleral region when wearing soft<sup>29</sup> and scleral lenses<sup>9</sup> in both healthy<sup>9,29</sup> and also compromised eyes.<sup>30</sup> The ESP provides an RMS error of  $< 10 \mu\text{m}$  for the central 8 mm area of a calibrated artificial surface and  $< 40 \mu\text{m}$  for an extended measurement area of 16 mm.<sup>28</sup>

Although the importance of scleral topography for an optimal contact lens fit has been recognized, traditionally works in scleral topography were restricted to assessing a few isolated scleral points.<sup>3,4</sup> This work presents a low-variance, automatic method based on 3D topography to grade scleral asymmetry. Even though further work is necessary to ensure the validity of this methodology in compromised eyes, such a grading system could assist practitioners in scleral lens fitting.

A limitation of the study was the use of a single lens design, necessitating additional work to investigate the influence of contact lens design. Due to the growth in clinical practice of toric haptic scleral lenses it would be of interest investigating whether the phenomena reported in this work are also observable when wearing toric scleral lenses. Similarly, all study participants were young, in good ocular health, and wore the miniscleral lens only once for a relatively short-term period. Longer studies on both healthy and compromised eyes could further help to elaborate the full effect of these lenses exert on the anterior surface.

In conclusion, miniscleral contact lenses do not set uniformly on the ocular surface. Scleral asymmetry showed its potential to be used as a parameter to predict lens settling on the eye. Larger scleral asymmetry leads to more lens decentration, with the largest decentration found in the horizontal meridian. This objective and accurate method could help practitioners prevent cases of scleral blanching or discomfort due to an excessive compression of the lens.

## REFERENCES

1. Visser ES, Visser R, van Lier HJ, Otten HM. Modern scleral lenses part II: patient satisfaction. *Eye Contact Lens* 2007; 33: 21-25.
2. Vincent SJ. The Rigid Lens Renaissance: A Surge in Sclerals. *Cont Lens Anterior Eye* 2018; 41: 139-143.
3. Ritzmann M, Caroline PJ, Börret R, Korszen E. An analysis of anterior scleral shape and its role in the design and fitting of scleral contact lenses. *Cont Lens Anterior Eye* 2018; 41: 205-213.
4. Bandlitz S, Baumer J, Conrad U, Wolffsohn J. Scleral topography analysed by optical coherence tomography. *Cont Lens Anterior Eye* 2017; 40: 242-247.
5. Consejo A, Rozema JJ. Scleral Shape and Its Correlations With Corneal Astigmatism. *Cornea* 2018; 37: 1047-1052.
6. Consejo A, Llorens-Quintana C, Bartuzel MM, Iskander DR, Rozema JJ. Rotation asymmetry of the human sclera. *Acta Ophthalmol* 2018 (in press, 10.1111/aos.13901).
7. Walker MK, Bergmanson JP, Miller WL, Marsack JD, Johnson LA. Complications and fitting challenges associated with scleral contact lenses: A review. *Cont Lens Anterior Eye* 2016; 39: 88-96.
8. Alonso-Caneiro D, Vincent SJ, Collins MJ. Morphological changes in the conjunctiva, episclera and sclera following short-term miniscleral contact lens wear in rigid lens neophytes. *Cont Lens Anterior Eye* 2016; 39: 53-61.
9. Consejo A, Behaegel J, Van Hoey M, Wolffsohn JS, Rozema JJ, Iskander DR. Anterior eye surface changes following miniscleral contact lens wear. *Cont Lens Anterior Eye*. 2018 (doi.org/10.1016/j.clae.2018.06.005).
10. Vincent SJ, Kowalski LP, Alonso-Caneiro D, Kricancic H, Collins MJ. The influence of centre thickness on miniscleral lens flexure. *Cont Lens Anterior Eye* 2018. (doi.org/10.1016/j.clae.2018.07.003)
11. Vincent SJ, Alonso-Caneiro D, Collins MJ. The temporal dynamics of miniscleral contact lenses: Central corneal clearance and centration. *Cont Lens Anterior Eye* 2017; 41: 162-168.
12. Ticak A, Marsack JD, Koenig DE, Ravikumar A, Shi Y, Nguyen LC, et al. A Comparison of Three Methods to Increase Scleral Contact Lens On-Eye Stability. *Eye Contact Lens* 2015; 41: 386-390.
13. Read SA, Collins MJ, Carney LG. The diurnal variation of corneal topography and aberrations. *Cornea* 2005; 24: 678-87.
14. Consejo A, Radhakrishnan H, Iskander DR. Scleral changes with accommodation. *Ophthalmic Physiol Opt* 2017; 37: 263-274.
15. Consejo A, Iskander DR. Corneo-scleral limbus demarcation from 3D height data. *Contact Lens and Anterior Eye* 2016; 39: 450-457.
16. Consejo A, Llorens-Quintana C, Radhakrishnan H, Iskander DR. Mean shape of the human limbus. *J Cataract Refract Surg* 2017; 43: 667-672.
17. Visser ES, Van der Linden BJ, Otten HM, Van der Lelij A, Visser R. Medical applications and outcomes of bitangential scleral lenses. *Optom Vis Sci* 2013; 90: 1078-1085.
18. Esen F, Toker E. Influence of Apical Clearance on Mini-Scleral Lens Settling, Clinical Performance, and Corneal Thickness Changes. *Eye Contact Lens* 2017; 43: 230-235.
19. Bray C, Britton S, Yeung D, Haines L, Sorbara L. Change in over-refraction after scleral lens settling on average corneas. *Ophthalmic Physiol Opt* 2017; 37: 467-472.

20. Severinsky B, Behrman S, Frucht-Pery J, Solomon A. Scleral contact lenses for visual rehabilitation after penetrating keratoplasty: long term outcomes. *Cont Lens Anterior Eye* 2014; 37: 196-202.
21. Pecego M, Barnett M, Mannis MJ, Durbin-Johnson B. Jupiter Scleral Lenses: the UC Davis Eye Center experience. *Eye Contact Lens* 2012; 38: 179-182.
22. Jones L, Brennan NA, González-Méijome J, Lally J, Maldonado-Codina C, Schmidt TA, et al. The TFOS International Workshop on Contact Lens Discomfort: Report of the contact lens materials, design, and care subcommittee TFOS International Workshop on CLD. *Invest Ophthalmol Vis Sci* 2013; 54: TFOS37-TFOS70.
23. Fadel D. The influence of limbal and scleral shape on scleral lens design. *Cont Lens Anterior Eye* 2018; 41: 321-328.
24. Soeters N, Visser ES, Imhof SM, Tahzib NG. Scleral lens influence on corneal curvature and pachymetry in keratoconus patients. *Cont Lens Anterior Eye* 2015; 38: 294-297.
25. Vincent SJ, Alonso-Caneiro D, Collins MJ. Corneal changes following short-term miniscleral contact lens wear. *Cont Lens Anterior Eye* 2014; 37: 461-468.
26. Vincent SJ, Alonso-Caneiro D, Collins MJ. Miniscleral lens wear influences corneal curvature and optics. *Ophthalmic Physiol Opt* 2016; 36: 100-111.
27. Vincent SJ, Alonso-Caneiro D, Collins MJ, Beanland A, Lam L, Lim CC, et al. Hypoxic Corneal Changes following Eight Hours of Scleral Contact Lens Wear. *Optom Vis Sci* 2016; 93: 293-299.
28. Iskander DR, Wachel P, Simpson PN, Consejo A, Jesus DA. Principles of operation, accuracy and precision of an Eye Surface Profiler. *Ophthalmic Physiol Opt* 2016; 36: 266-278.
29. Consejo A, Bartuzel MM, Iskander DR. Corneo-scleral limbal changes following short-term soft contact lens wear. *Cont Lens Anterior Eye* 2017; 40: 293-300.
30. Piñero DP, Soto-Negro R. Anterior Eye Profilometry-guided Scleral Contact Lens Fitting in Keratoconus. *Int J Kerat Ect Cor Dis* 2017; 6: 97-100.